INTERNATIONAL JOURNAL ON SMART SENSING AND INTELLIGENT SYSTEMS VOL. 7, NO. 3, SEPTEMBER 2014

www.s2is.org
International Journal on Smart Sensing and Intelligent Systems
ISSN 1178-5608

RESEARCH ON LQR ZONE CONTROL ALGORITHM FOR PICKING ROBOT ARM

[1]Zhang Zhiyong, [1*] Huang Lvwen, [1]Xu Yang, [1]Zhang Xiaoting

1,College of information Engineering

Northwest A&F University, Yangling, Shaanxi, 712100, China

E-mail: zzy@nwsuaf.edu.cn,

Submitted: May 3, 2014 ***Accepted: July 10, 2014*** ***Published: Sep. 1, 2014***

Abstract- This paper aims at improve the poor stability and the fluttering problems on picking apples for picking robot arm, we establish the dynamics model of Picking Robot Arm using Lagrange equation and divide the whole movement space of Picking Robot Arm into stretch area and picking area by analyzing the dynamic model. Making full using of the model, we put forward to the strategy based on the extension energy control and LQR Zone control. Furthermore, we solve the problem on ensuring the picking robot arm's energy increasing for the picking stretch process. The energy stability control study on establishing the robust performance analysis and design in theory lays a foundation for other relevant stability study.

Index terms: Picking Robot Arm, the zone control, dynamic model, LQR.

I. INTRODUCTION

It is necessary to control the contact force applied to picking environment at the contact point, fluttering control is required when using a flexible arm for such a complex picking task. Furthermore link flexibility may contribute to the instability problem in arm control. Many researchers have investigated the fluttering control of picking arms based on a finite-dimensional approximated model [1–2]; this has meant, however, that the findings obtained in these studies are confined to the finite-dimensional approximated model. The dimension of the controller increases along with an increase in the number of modes provided in the controller design model. Furthermore, fluttering, which results from a neglected high-frequency characteristic, makes such systems unstable. For these reasons, it is both desirable and of interest to consider the force control of a flexible arm using the infinite dimensional model. In contrast to investigations based on the finite-dimensional approximated model, there are only a few studies based on the infinite dimensional model.

At present, many control methods such as Variable structure control, Adaptive control, Singular perturbation control et al. has been applied in picking robot arm stability control area. It is difficult to meet the requirements of system control only through a control strategy due to the characteristics of arm length, wide range of motion, multiple joint and multiple degrees of freedom for picking apples [3]. Based on the analysis of characteristics of the joint movement which alike man's gripper, we adopt the different tactics to achieve partition control to make the picking robot arm reach apple picking area stably and pick the ripe apple without fluttering according to the joint torque and rotation angle. It can be provided theoretical reference and technological reference for relevant control problems. In the kinematics of picking robot arm, we also can calculate each joint turning angle by solving motion equations according to the position of picking gripper while it reaching the picking area. So each joint movement is not independent, but connected and coordinated. Actually the picking movement of picking robot arm is controlled respectively by their own joint axis servo, so the picking movement must be decomposed to the velocity, acceleration, force of joint axis, the actuators moment must be broken down into the speed, acceleration, force or moment of joint shaft, and be completed the movement by independent control servo system of each joint. However, the servo control system often is completed in the joint coordinate system. According to the experience of the related majority literature [4-6], we usually apply the Cartesian coordinates to indicate the end actuator position, so it is necessary to control motion parameters including velocity, acceleration and force (torque) of the movement decomposition.

(1) Speed control of movement decomposition

In order to ensure picking robot arm joint stable operation in the Cartesian axes, the speed control needs to drive joint motors joint run with the respective real-time velocity at the same time. During the control of movement decomposition, firstly we gain the expected joint velocity by decomposing the Descartes position, and then implement the stability control of servo. In Cartesian coordinates, the position of 3-DOF picking robot arm can be represented as

$$X(t)=\begin{bmatrix}P_X & P_Y & P_Z & \psi & \theta & \Phi\end{bmatrix}^T \qquad (1)$$

But the generalized coordinate vector is also represented

$$q(t)=\begin{bmatrix}q_1 & q_2 & \dots & q_n\end{bmatrix}^T \qquad (2)$$

The relation between equation (1) and equation (2) can be represented as

$$X(t)=f(q) \qquad (3)$$

The relationship of the joint angle and the Cartesian coordinate can be expressed in equation (3), then derivations equation (3), we can gain

$$\dot{X}(t)=J(q)\dot{q}(t) \qquad (4)$$

Where $J(q)$ denotes generalized Jacobi matrix, $\dot{X}(t)$ denotes expectations speed of picking arms in Cartesian coordinates, $\dot{q}(t)$ denotes the joint speed in joint space.

$$J_{ij}=\frac{\partial f_i}{\partial q_i}(1\le i\le m,1\le j\le m) \qquad (5)$$

equation (5) represents the corresponding relations on two kinds of speed, we could should discuss the relation about the freedom degree m and the space movement freedom degree n in order to get the mathematical expression of $\dot{q}(t)$ corresponding to the $\dot{X}(t)$. If m=n which denotes the picking robot arm freedom degree and the picking space freedom degree are equal, picking robot arm freedom degree is redundant, and we can solve the inverse matrix of its Jacobi matrix directly

$$\dot{q}(t)=J^{-1}(q)\dot{X}(t) \qquad (6)$$

If m<n, which represents that picking robot arm have not the redundant freedom degree, we can solve its generalized inverse matrix

$$\dot{q}(t) = J^{+}(q)\dot{X}(t) \qquad (7)$$

Where, $J^{+}(q)$ denotes generalized inverse matrix equation (7) is the least squares solution of equation (6), if $J(q)$ is a full rank matrix, then there exist following equation

$$\boldsymbol{J}^{+}(\boldsymbol{q}) = \boldsymbol{J}(\boldsymbol{q})^{\mathrm{T}}[\boldsymbol{J}(\boldsymbol{q})\boldsymbol{J}(\boldsymbol{q})^{\mathrm{T}}]^{-1} \qquad (8)$$

According to equation (7), the solution of $J^{+}(q)$ can simplify following equation.

$$J^{+} = J^{T}(JJ^{T})^{-1} \qquad (9)$$

Equation (6) and equation (7) represent picking robot arm joint velocity respectively on the condition of redundancy and non-redundancy. We can structure the picking robot arm motion control scheme according to these two equations and decompose the picking robot arm movement into the joint movement. So the control method is referred to speed control of movement decomposition.

(2) Acceleration control of movement decomposition

The acceleration control of movement decomposition is the extensiveness of the speed control. Its method is that we can decompose the acceleration in the Cartesian coordinates into the corresponding joint acceleration, then we can solve the control moment which apply to the joint motor according to the corresponding system dynamics model. By solving the derivative of equation (6), we can gain the picking robot arm acceleration

$$\ddot{X}(t) = J(t)\ddot{q}(t) + \dot{J}\dot{q}(t) \qquad (10)$$

Equation (10) represents the corresponding acceleration relations in the Cartesian coordinates and the joint coordinate system, namely the decomposition control of the desired acceleration in the Cartesian coordinates. The target of acceleration control is virtually to make the precision error between the trajectory and the desired position evaluation converge to zero, now assuming that

$$e = X_d - X \qquad (11)$$

Where, e denotes the precision error between the actual position and the desired evaluation position, X_d denotes the desired position vector , X denotes the actual position vector. In order to make the desired evaluation converge to zero, the following relations must be satisfied

$$\ddot{e} + k_1\dot{e} + k_2 e = 0 \qquad (12)$$

Where k_1,k_2 denote the ratio coefficient. The value of the ratio coefficient should make the characteristic root of the real part be negative. Substituting the equation (10) and equation (11) into the equation (12), we can gain

$$\ddot{q}(t) = -k_1\dot{q}(t) + J^{-1}(q)[\ddot{X}(t) + k_1\dot{X}_d(t) + k_2 e(t) - \dot{J}(q,\dot{q})]\dot{q}(t) \qquad \textbf{(13)}$$

The equation (13) is the theoretical basis on acceleration control of movement decomposition for closed-loop picking robot arm control. If the path of the picking robot arm in the Cartesian coordinates is planned in advanced, the desired position, speed and acceleration of the end actuator in this coordinate system are known. Then we can calculate the acceleration in the joint coordinate system. Making full using of the speed and acceleration of picking robot arm joint and its dynamic equation, we can calculate the force or torque belonged to picking robot arm join. According to dynamic principle [4-7], we can gain the picking robot arm dynamic equation

$$M(q)\ddot{q} + H(q,\dot{q})\dot{q} + G(q) = \tau \qquad \textbf{(14)}$$

Where $M(q)$ denotes inertia matrix of picking robot arm, $H(q,\dot{q})$ denote Centrifugal force and force vector, $G(q)$ denotes gravity vector, τ denotes force and torque vector applying to picking robot arm joint.

(3) Force and torque control

The basic idea on the force and torque control of the movement decomposition is that we calculate the control torque applied to driven joint firstly and then control the position and speed of the picking gripper in the Cartesian coordinates. The theory basis of force and torque control is the dynamical model and the method is the solution of inverse dynamics. Given that force and torque control in the arm joint space is closed loop according to the desired gripper, its position in the Cartesian coordinates is also known, we can gain its corresponding desired position q_d in the joint coordinate system by kinematics calculation and we can also gain the position error in the arm joint space q

$$e_q = q_d - q \qquad \textbf{(15)}$$

In order to make the error between the actual trajectory and the expectation trajectory of picking robot arm joint space decreases in the process of joint movement until convergence is zero, the error should be satisfied

$$\ddot{e}_q + k_{1q}\dot{e}_q + k_{2q}e_q = 0 \qquad \textbf{(16)}$$

At the same time, the coefficient of k_{1q} and k_{2q} should be a positive and the characteristic root of equation (16) should be located in the negative half plane. Substituting the equation (15) and equation (16) into the equation (14), we can gain the following

$$\tau = M(q)(\ddot{q}_d - k_{1q}\dot{e}_q - k_{2q}e_q) + H(q,\dot{q})\dot{q} + G(q) \qquad (17)$$

Equation(17) represent the calculation method of the force and moment in the control process of picking robot arm.

II. PICKING ROBOT ARM DYNAMICS MODEL EQUATION

There are some methods of Studying of picking robot arm dynamics such as Lagrange method, Newton-Euler method, Gauss method, Roberon-Wittenburg method and Kane method and so on [8,9], all of these methods are benefit to the control of picking robot arm. Lagrange equation is suitable for the mathematical modeling and simulation of dynamics and kinematics analysis, because of its mechanical dynamic characteristics owns the characteristics of multi-movement and multi-freedom degree, it is especially applied in the robot motion mechanics based on the multi-body dynamics. So we research the picking robot arm dynamics by using Lagrange equation.

(1) Lagrange equation of picking robot arm

Research literature [9-10] represented that the dynamic equation based on Lagrange theory is applied to the study of arm dynamic model, its derivation process is simple, and it can clearly represent the coupling characteristic of arms, and can also directly represent the system control input function. Therefore we can establish the dynamics equation by using the recursive Lagrange equation in the form of homogeneous coordinates. For any mechanical system, the Lagrange method establishing the dynamics equation based on the system of kinetic energy and potential energy, and this method can avoid mechanism motion analysis. Using the difference between the total kinetic energy E_k and potential energy E_P, we can establish the system Lagrange function L and its concise dynamic equation [11-12]

$$L = E_K - E_P \qquad (18)$$

$$F_i = \frac{d}{dt}\left(\frac{\partial L}{\partial \dot{q}_i}\right) - \frac{\partial L}{\partial q_i} \, (i = 1,2,3) \qquad (19)$$

Where L denotes Lagrange function, n denotes the arm number q_i denotes the selected system generalized coordinate, which unit is m or rad depending on its linear coordinate or angle coordinate, $\dot{q}_i$ denotes the generalized velocity ,the first order derivative is the generalized coordinates q_i to the time, which unit is m/s or rad/s depending on the selected system generalized coordinate is linear coordinate or Angle coordinate, F_i denotes the generalized force or generalized moment acting on the i coordinate [13]. For the equation (19) does not involve $\dot{q}_i$, it can be written as

$$F_i = \frac{d}{dt}\frac{\partial L_k}{\partial \dot{q}_i} - \frac{\partial E_K}{\partial q_i} + \frac{\partial E_P}{\partial q_i} \qquad (20)$$

Where 1) The kinetic energy of the system E_k is a function to q_i, $\dot{q}_i$ and the time t, but the system potential energy E_P is just the function to q_i, so the Lagrange function can be written $L = L(q_i, \dot{q}_i, t)$ 2) If q_i is the angular displacement, $\dot{q}_i$ is the angular velocity and the corresponding F_i is the torque, If q_i is the linear displacement, $\dot{q}_i$ is the linear velocity and the corresponding F_i is the force. In this paper, the q_i is the angular displacement, so the F_i is the torque.

(2) Dynamics analysis of picking robot arms

Picking robot arm are a complex, nonlinear and multi parameter coupling dynamics systems. Solving the dynamic problems need a long operation time, so solving simply picking robot arm dynamics and reducing the online computation time are long-term focused on research target in the field of dynamics [14]. The dynamics problem own two styles

1) Using the θ_i, $\dot{\theta}_i$ and $\ddot{\theta}_i$ of the known trajectory point, namely the angular position and angular velocity and angular acceleration of the picking robot arm joints , we can gain the corresponding joint vector matrix τ .

2) Using the joint driving moment, we can gain the corresponding instantaneous picking robot arm movement. Namely, we can gain the θ_i, $\dot{\theta}_i$ and $\ddot{\theta}_i$ of the picking robot arm joints making full use of joint vector matrix τ [15].

(3). Establishment the picking robot arm dynamics equation

As a complex system, we generally adopt the homogeneous transformation to set up the system dynamics equation by using the Lagrange equation and describe its pose and motion state. Now, we can study the derivation process of dynamics equation referring to Figure 1. The system variables definition and experimental parameters are shown in table 1. On the convenience of research, we make the following assumptions

1) Picking robot arm are rigid bodies, the control objects input is just the output torque of the joint motor.

2) Ignoring air resistance and various frictions.

3) Part between the shoulder and elbow called the upper arm and part between elbow and wrist joints is called the forearm can all be abstracted to homogeneous bar.

Table.1 The parameters of picking robot arm

Upper arm	**Quantity**	**Forearm**	**Quantity**	**Picking gripper**	**Quantity**
Mass m_1 （kg）	2.6	Mass m_2 （kg）	1.95	Mass m_3 （kg）	0.65
Length l_1 （m）	1.08	Length l_2 （m）	0.69	Length l_3 （m）	0.20
Distance between center upper arm and shoulder joint l_{c1} （m）	0.54	distance between center forearm and elbow joint l_{c2} （m）	0.145	Distance between center picking gripper and wrist join l_{c3} （m）	0.06
Moment of inertia I_{c1} （kg.m^2）	2.2×10^{-1}	Moment of inertia I_{c2} （kg.m^2）	0.77×10^{-1}	Moment of inertia I_{c3} （kg.m^2）	0.21×10^{-2}

Based on the above assumptions and other references [16], we can gain the method by establishing arm dynamics equation.

Firstly, Selecting the coordinate system and the completely independent generalized joint variables q_i (i=1, 2, ..., n), then determine the corresponding generalized force F_i on the joints . If q_i is the linear displacement, the corresponding F_i is the force, and if q_i is the angular displacement, the corresponding F_i is the torque, lastly, solving the kinetic energy and potential

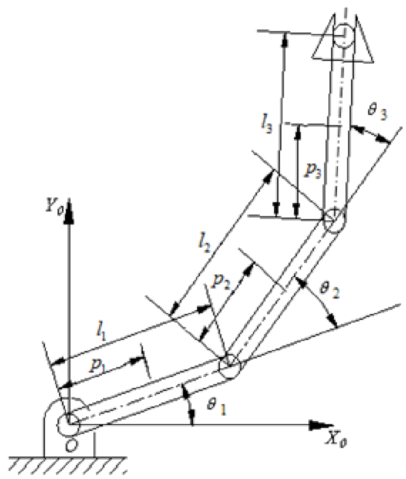

Figure.1 The diagram of 3-DOF dynamics for picking robot arm

energy for picking robot arm, constructing the dynamic equations of the arm system. The specific derivation steps are executed as following

1) Selecting generalized joint variables and generalized force

In Cartesian coordinate, τ_1 is the elbow torque, τ_2 is the wrist joint torque, p_1 , p_2 , p_3 is respectively, the distance between the upper arm, forearm and the picking gripper to the centre of the joints. The definition of the rest of the parameters is shown in Table 1. So the centroid coordinates of the upper arm k_1 is described as

$$\begin{cases} X_1 = p_1 sin(\theta_1) \\ Y_1 = -p_1 \cos(\theta_1) \end{cases} \tag{21}$$

The speed square of the upper arm k_1

$$\dot{X}_1^2 + \dot{Y}_1^2 = \dot{p}_1^2$$

The centroid coordinates of the forearm k_2 is described as

$$\begin{cases} X_2 = l_1 \sin\theta_1 + p_2 \sin\theta_2 \\ Y_2 = -l_1 \cos\theta_1 - p_2 \cos\theta_2 \end{cases} \tag{22}$$

The speed's square of the forearm k_2

$$\begin{cases} \dot{X}_2 = l_1 \cos\theta_1\dot{\theta}_1 - p_2 \cos\theta_2\dot{\theta}_2 \\ \dot{Y}_2 = l_1 \sin\theta_1\dot{\theta}_1 + p_2 \sin\theta_2\dot{\theta}_2 \end{cases} \tag{23}$$

$$\dot{X}_2^2 + \dot{Y}_2^2 = l_1^2 c\theta_1\dot{\theta}_1^2 + p_2^2\left(\dot{\theta}_1 + \dot{\theta}_2\right)^2 + 2p_2 l_1\left(\dot{\theta}_1^2 + \dot{\theta}_2\dot{\theta}_1\right)c\theta_2$$

The centroid coordinates of the mass center of picking gripper k_3 is described as

$$\begin{cases} X_2 = l_1 \sin\theta_1 + l_2 \sin\theta_2 + p_3 \sin\theta_3 \\ Y_3 = -l_1 \cos\theta_1 - l_2 \cos\theta_2 - p_3 \cos\theta_3 \end{cases} \quad (24)$$

The speed's square of the mass center of picking gripper k_3 is

$$\begin{cases} \dot{X}_3 = l_1 \cos\theta_1 \dot{\theta}_1 - l_2 \cos\theta_2 \left(\dot{\theta}_1 + \dot{\theta}_2\right) + p_3 \cos\theta_3 (\dot{\theta}_1 + \dot{\theta}_2 + \dot{\theta}_3) \\ \dot{Y}_3 = l_1 \sin\theta_1 \dot{\theta}_1 + l_2 \sin\theta_2 \left(\dot{\theta}_1 + \dot{\theta}_2\right) + p_3 \sin\theta_3 (\dot{\theta}_1 + \dot{\theta}_2 + \dot{\theta}_3) \end{cases} \quad (25)$$

$$\dot{X}_3^2 + \dot{Y}_3^2 = l_1^2 \cos\theta_1 \dot{\theta}_1^2 + l_2^2 \left(\dot{\theta}_1 + \dot{\theta}_2\right)^2 + 2 l_2 l_1 \left(\dot{\theta}_1^2 + \dot{\theta}_2 \dot{\theta}_1\right) \cos\theta_2 + 3 p_3 l_1 l_2 \left(\dot{\theta}_1^2 + \dot{\theta}_2 \dot{\theta}_1 + \dot{\theta}_3^2\right) \cos\theta_2$$

2) Solving the system's kinetic energy

$$E_k = \sum E_{ki} (i = 1,2,3) \quad (26)$$

$$\begin{cases} E_{k1} = \frac{1}{2} m_1 p_1^2 \dot{\theta}_1^2 \\ E_{k2} = \frac{1}{2} m_2 l_1^2 \dot{\theta}_1^2 + \frac{1}{2} m_2 p_2^2 (\dot{\theta}_1^2 + \dot{\theta}_{21})^2 + m_2 l_2 p_2 (\dot{\theta}_1^2 + \dot{\theta}_1 \dot{\theta}_2) \cos\theta_2 \\ E_{k3} = \frac{1}{2} m_2 (l_1^2 \cos\theta_1 \dot{\theta}_1^2 + l_2^2 \left(\dot{\theta}_1 + \dot{\theta}_2\right)^2 + 2 l_2 l_1 \left(\dot{\theta}_1^2 + \dot{\theta}_2 \dot{\theta}_1\right) \cos\theta_2 + 3 p_3 l_1 l_2 \left(\dot{\theta}_1^2 + \dot{\theta}_2 \dot{\theta}_1 + \dot{\theta}_3^2\right) \cos\theta_2) \end{cases}$$

3) Solving the system potential energy

$$E_p = \sum E_{pi} (i = 1,2,3) \quad (27)$$

$$\begin{cases} E_{p1} = m_1 g p_1 (1 - \cos\theta_1) \\ E_{p2} = m_1 g l_1 (1 - \cos\theta_1) + m_2 g p_2 (1 - \cos\theta_2) \\ E_{p3} = m_1 g l_1 (1 - \cos\theta_1) + m_2 g l_2 (1 - \cos\theta_2) + m_2 g p_2 (1 - \cos\theta_3) \end{cases}$$

4) Solving the system research function

$$\begin{aligned} L &= E_k - E_p = E_{k_1} + E_{k_2} + E_{k_3} - (E_{p_1} + E_{p_2} + E_{p_3}) \\ &= \frac{1}{2} m_2 (l_1^2 \cos\theta_1 \dot{\theta}_1^2 + l_2^2 \left(\dot{\theta}_1 + \dot{\theta}_2\right)^2 + 2 l_2 l_1 \left(\dot{\theta}_1^2 + \dot{\theta}_2 \dot{\theta}_1\right) \cos\theta_2 + 3 p_3 l_1 l_2 \left(\dot{\theta}_1^2 + \dot{\theta}_2 \dot{\theta}_1 + \dot{\theta}_3^2\right) \cos\theta_2) \\ &- m_2 p_2 g (1 - c\theta_{12}) + \frac{1}{2} (m_1 p_1^2 + m_2 l_1^2) \dot{\theta}_1^2 + m_2 l_1 p_2 (\dot{\theta}_1^2 + \dot{\theta}_1 \dot{\theta}_2) c\theta_2 + \frac{1}{2} m_2 p_2^2 (\dot{\theta}_1 + \dot{\theta}_2)^2 \\ &- (m_1 p_1 + m_2 l_1) g (1 - cos\theta_1) - m_1 g l_1 (1 - \cos\theta_1) + m_2 g l_2 (1 - \cos\theta_2) + m_2 g p_2 (1 - \cos\theta_3) \end{aligned}$$

5) Solving the System dynamics equation

We can calculate the torque represent joint and the dynamics equation of the control system for picking robot arm by the equation (20).

a. The forearm torque τ_1

$$\begin{aligned}\frac{\partial L}{\partial \dot{\theta}_1} &= (m_1 p_1{}^2 + m_2 l_1{}^2)\dot{\theta}_1^2 + (m_2 p_2{}^2 + m_3 l_2{}^2)\dot{\theta}_2^2 + (m_3 p_3{}^2 + m_2 l_1{}^2 + m_1 l_2{}^2)\dot{\theta}_3^2 \\ &+ m_2 l_1 p_2 (2\dot{\theta}_1^2 + \dot{\theta}_2 + \dot{\theta}_3) c\cos\theta_2 + m_1 l_1 p_2 (3\dot{\theta}_1^2 + \dot{\theta}_2)\cos\theta_3 \\ &+ m_2 p_2{}^2 (2\dot{\theta}_3 + \dot{\theta}_2) + m_3 p_3{}^2 (2\dot{\theta}_1 + \dot{\theta}_2 + \dot{\theta}_3)\end{aligned} \quad (28)$$

$$\frac{\partial L}{\partial \theta_1} = -(m_1 p_1 + m_2 p_2 + m_3 l_1^2) g \sin\theta_1 + (m_3 p_3 + m_2 l_1^2) g\cos\theta_3 - m_2 g p_2 \sin\theta_2 \quad (29)$$

So

$$\begin{aligned}\tau_1 &= \frac{d}{dt}\frac{\partial L}{\partial \dot{\theta}_1} - \frac{\partial L}{\partial \theta_1} \\ &= D_{11}\ddot{\theta}_1 + D_{12}\ddot{\theta}_2 + D_{13}\ddot{\theta}_3 + D_{111}\dot{\theta}_1^2 + \\ & D_{122}\dot{\theta}_2^2 + D_{133}\dot{\theta}_3^2 + 2D_{112}\dot{\theta}_1\dot{\theta}_2 + 2D_{113}\dot{\theta}_1\dot{\theta}_3 + 2D_{123}\dot{\theta}_2\dot{\theta}_3 + D_1\end{aligned} \quad (30)$$

$$\begin{cases} \mathrm{D}_{11} = m_1 p_1{}^2 + m_2 p_2{}^2 + m_2 l_1{}^2 + 2m_2 l_1 p_2 c\theta_2 \\ \mathrm{D}_{12} = m_2 p_2{}^2 + m_2 l_1 p_2 c\theta_2 \\ \mathrm{D}_{112} = -2m_2 l_1 p_2 s\theta_2 \\ \mathrm{D}_{122} - m_2 l_1 p_2 s\theta_2 \\ \mathrm{D}_1 = (m_1 p_1 + m_2 l_1) g s\theta_1 + m_2 p_2 g s_{12} \end{cases} \quad \begin{cases} \mathrm{D}_{13} = m_1 p_1{}^2 + m_2 l_1{}^2 + 2m_2 l_1 p_2 c\theta_2 + 2m_3 l_1 p_2 c\theta_3 \\ \mathrm{D}_{111} = m_2 p_2{}^2 + m_2 l_1 p_2 c\theta_2 + m_3 l_1 p_3 \cos\theta_3 \\ \mathrm{D}_{113} = -2m_2 l_1 p_2 s\theta_2 - 2m_3 l_2 p_1 \sin\theta_1 \\ \mathrm{D}_{133} = -m_2 l_1 p_2 s\theta_2 - m_1 l_2 p_2 s\theta_3 \\ \mathrm{D}_{112} = (m_1 p_1 + m_2 l_1 + m_3 l_2) g\sin\theta_1 + m_3 p_2 g\sin\theta_3 \end{cases} \quad (31)$$

b The upper arm torque τ_2

$$\frac{\partial L}{\partial \dot{\theta}_2} = m_2 p_2{}^2 (\dot{\theta}_1 + \dot{\theta}_2 + \dot{\theta}_3) + m_1 p_2{}^2 (2\dot{\theta}_1 + \dot{\theta}_2 \text{-} 3\dot{\theta}_3) + m_3 l_1 p_2 \dot{\theta}_1 c\cos\theta_2 + m_2 l_3 p_1 \dot{\theta}_2 c\cos\theta_3 \quad (32)$$

$$\frac{\partial L}{\partial \theta_2} = -m_2 l_1 p_2 (\dot{\theta}_1^2 + \dot{\theta}_1\dot{\theta}_2 + \dot{\theta}_2\dot{\theta}_3)\cos\theta_2 + m_3 l_2 p_1 (\dot{\theta}_2^2 + \dot{\theta}_2\dot{\theta}_3)\cos\theta_3 - m_2 g p_2 s_{12} \quad (33)$$

So

$$\begin{aligned}\tau_2 &= \frac{d}{dt}\frac{\partial L}{\partial \dot{\theta}_2} - \frac{\partial L}{\partial \theta_2} \\ &= D_{21}\ddot{\theta}_1 + D_{22}\ddot{\theta}_2 + D_{23}\ddot{\theta}_3 + D_{211}\dot{\theta}_1^2 + D_{222}\dot{\theta}_2^2 + D_{233}\dot{\theta}_3^2 \\ &+ 2D_{212}\dot{\theta}_1\dot{\theta}_2 + 2D_{213}\dot{\theta}_1\dot{\theta}_3 + 2D_{223}\dot{\theta}_2\dot{\theta}_3 + D_2\end{aligned} \quad 34)$$

During the equation

$$\begin{cases} D_{21} = m_2 p_2{}^2 + m_2 l_1 p_2 c\theta_2 \\ D_{22} = m_2 p_2{}^2 \\ D_{212} = -m_2 l_1 p_2 s\theta_2 + m_2 l_1 p_2 s\theta_2 = 0 \\ D_{211} = m_2 l_1 p_2 s\theta_2 \\ D_2 = m_2 g p_2 s_{12} \end{cases} \quad \begin{cases} \mathrm{D}_{23} = m_2 p_1{}^2 + m_3 p_3{}^2 + m_2 l_1{}^2 + 2 m_2 l_1 p_2 \cos\theta_1 \cos\theta_2 \\ \mathrm{D}_{211} = m_2 p_2{}^2 + m_3 l_2 p_2 \cos\theta_2 \cos\theta_3 \\ \mathrm{D}_{213} = -2 m_2 l_1 p_2 \sin\theta_2 + 3 m_3 l_1 p_3 \sin\theta_2 \sin\theta_3 \\ \mathrm{D}_{233} - m_2 l_1 p_2 \sin\theta_2 \sin\theta_3 \\ \mathrm{D}_{212} = (m_1 p_1 + m_2 l_1) g s\theta_1 + m_3 p_3 g \sin\theta_1 \end{cases} \tag{35}$$

c. The picking grippers torque τ_3

$$\frac{\partial L}{\partial \dot{\theta}_3} = m_1 p_2{}^2 (\dot{\theta}_2^2 + 2\dot{\theta}_1\dot{\theta}_3 + \dot{\theta}_2\dot{\theta}_3) + m_3 l_1 p_2 \dot{\theta}_1 \cos\theta_3 \tag{36}$$

$$\frac{\partial L}{\partial \theta_2} = -m_2 l_1 p_2 (\dot{\theta}_1{}^2 + \dot{\theta}_1\dot{\theta}_2) c\theta_2 + m_1 l_2 p_2 (\dot{\theta}_2{}^2 + 2\dot{\theta}_1\dot{\theta}_2) \sin\theta_2 - m_2 g p_2 \sin\theta_3 \tag{37}$$

So

$$\begin{aligned} \tau_3 &= \frac{d}{dt}\frac{\partial L}{\partial \dot{\theta}_3} - \frac{\partial L}{\partial \theta_3} \\ &= D_{31}\ddot{\theta}_1 + D_{32}\ddot{\theta}_2 + D_{33}\ddot{\theta}_3 + D_{311}\dot{\theta}_1^2 \\ &+ D_{322}\dot{\theta}_2^2 + D_{333}\dot{\theta}_3^2 + 2D_{312}\dot{\theta}_1\dot{\theta}_2 + 2D_{313}\dot{\theta}_1\dot{\theta}_3 + 2D_{323}\dot{\theta}_2\dot{\theta}_3 + D_3 \end{aligned} \tag{38}$$

Where

$$\begin{cases} D_{31} = m_2 p_2{}^2 + m_2 l_1 p_2 \cos\theta_2 + m_1 p_1{}^2 + m_3 l_1 p_2 \cos\theta_3 \\ D_{32} = m_2 p_2{}^2 + m_3 l_1 p_3^2 \\ D_{312} = -m_2 l_1 p_2 s\theta_2 + m_2 l_1 p_2 s\theta_2 + m_3 l_1 p_2 \sin\theta_3 \\ D_{311} = m_2 l_1 p_2 \sin\theta_2 - m_3 l_3 p_1 \sin\theta_3 \\ D_3 = m_2 g p_2 \sin\theta_2 + m_3 g p_2 \cos\theta_3 \end{cases} \quad \begin{cases} \mathrm{D}_{33} = m_1 p_1{}^2 + m_2 p_2{}^2 + m_2 l_1{}^2 + 2 m_3 l_2 p_2 \cos\theta_1 \\ \mathrm{D}_{311} = m_2 p_2{}^2 + 3 m_2 l_1 p_2 \cos\theta_2 \\ \mathrm{D}_{313} = -2 m_2 l_1 p_2 \sin\theta_2 \\ \mathrm{D}_{333} - m_2 l_1 p_2 \cos\theta_2 + m_2 p_2 g \sin\theta_3 \\ \mathrm{D}_{312} = (m_1 p_1 + m_2 l_1) g \sin\theta_1 + m_2 p_2 \cos\theta_2 \end{cases} \tag{39}$$

Equation (28), (29), (30), (31), (32), (35), (38), and (39) represent respectively the relationship between the displacement, velocity, acceleration of each joint and the joint driving moment. Namely, the relationship between the force and movement is called dynamics equation of picking robot arm. This is as following

1) Containing $\ddot{\theta}_1$, $\ddot{\theta}_2$ and $\ddot{\theta}_3$ are joint torques caused by acceleration, The D_{11},D_{22},D_{33} represent respectively the inertia moment in the equation, because of the shoulder joint acceleration, elbow and wrist joint acceleration . The D_{12} represents the coupling inertia moment that the elbow joint acceleration corresponding to shoulder joint acceleration, The D_{21} represents the coupling inertia moment that the shoulder joint acceleration corresponding to elbow joint acceleration.

2) Containing $\dot{\theta}_1^2$, $\dot{\theta}_2^2$ and $\dot{\theta}_3^2$ are joint torques caused by centripetal force, in the equations, the D_{122} represents the coupling inertia moment that the centripetal force caused by the elbow joint speed corresponding to shoulder joint, The D_{211} represents the coupling inertia moment that the centripetal force caused by the shoulder joint speed corresponding to elbow joint, The D_{322} represents the coupling inertia moment that the centripetal force caused by the elbow joint speed corresponding to wrist joint.

3) Containing $\dot{\theta}_1$ $\dot{\theta}_2$ $\dot{\theta}_3$ are joint torques caused by Coriolis force, in the equations, the D_{112} represent the coupling inertia moment that the Coriolis force corresponding to shoulder joint, the D_{212} represents the coupling inertia moment that the Coriolis force corresponding to elbow joint, the D_{213} represents the coupling inertia moment that the Coriolis force corresponding to wrist joint.

4) Containing $\dot{\theta}_1$, $\dot{\theta}_2$, $\dot{\theta}_3$ are joint torques caused by the force of gravity, in the equations, the D_1 represents the heavy torque that the quality of the upper arm and forearm corresponding to shoulder joint, the D_2 represents the heavy torque that the quality of the forearm corresponding to shoulder joint, the D_3 represents the heavy torque that the quality of the picking grippers corresponding to elbow joint.

By the above method, the dynamics equation of 3-DOF picking robot arm is relatively complex, it contains a variety of factors affecting the dynamic properties of picking robot arm. Due to the trivial derivation computation and the complex dynamics equation, it is not conducive to real-time control on the picking robot arm for multiple freedom degrees. Learned from the reference [17], we can simplify the heavy torque when the arm are short and light, we should omit the items containing $\dot{\theta}_1^2$, $\dot{\theta}_2^2$ and $\dot{\theta}_1, \dot{\theta}_2$ when the joints and the mass center velocity is not high , we should omit the items containing the $\ddot{\theta}_1^2$, $\ddot{\theta}_2^2$ and $\ddot{\theta}_3^2$ when the joints velocity is not high and operate smooth. Based on the simplified assumption and table 1, the equation (19) can be written as

$$J_i(\theta)\ddot{\theta}_i + c_i(\theta, \dot{\theta}) + g_i(\theta) = \tau \qquad (\mathbf{40})$$

Where $J_i(\theta)$ denotes the moment of inertia, $J_i(\theta)\ddot{\theta}_i$ denotes the inertia force, the symmetric and positive force definite matrices, $c_i(\theta, \dot{\theta})$ denotes the centrifugal force, $g_i(\theta)$ denotes the gravity applying on the picking robot arm. As there exit no external force for system ($\tau = 0$), we can apply the equation (30),(34) and (38) to derive the mathematical model

$$\frac{\mathrm{d}}{\mathrm{d}t}\left(\frac{\partial L}{\partial \dot{\theta}_i}\right) - \frac{\partial L}{\partial \theta_i} = 0 \qquad (41)$$

Apply the available deformation

$$J_i \ddot{\theta}_i + c_i + g_i = 0 \qquad (42)$$

Assuming that x_1 represent the center of mass velocity of the upper arm, x_2 represent the mass center velocity of the forearm, x_3 represent the mass center velocity of the picking gripper, x_4 represent the mass center acceleration of the upper arm, x_5 represent the mass center acceleration of the forearm, x_6 represent the mass center acceleration of the picking gripper. So the forearm centroid angular acceleration is $\dot{x}_5 = u_2$ and the upper arm centroid angular acceleration is $\dot{x}_4 = u_1$. After deducting the state vector space model and plugging the data, we can obtain the state space equation by solving simplify, we obtain the output equation of system

$$y = \dot{x} = \begin{vmatrix} 0 & 0 & 0 & 1 & 0 & 0 \\ 0 & 0 & 0 & 0 & 1 & 0 \\ 0 & 0 & 0 & 0 & 0 & 1 \\ 3.3089 & 11.6932 & -22.0632 & 0 & 0 & 0 \\ -37.2547 & -112.3976 & 44.8306 & 0 & 0 & 0 \\ 4.2986 & 182.8973 & 0.7907 & 0 & 0 & 0 \end{vmatrix} \begin{vmatrix} x_1 \\ x_2 \\ x_3 \\ x_4 \\ x_5 \\ x_6 \end{vmatrix} + \begin{vmatrix} 0 & 0 \\ 0 & 0 \\ 0 & 0 \\ 2.6897 & 5.6391 \\ -13.7438 & 19.1921 \\ 19.1921 & -12.6600 \end{vmatrix} \begin{vmatrix} u_1 \\ u_2 \end{vmatrix}$$

$$y = \dot{x} = \begin{vmatrix} 1 & 0 & 0 & 0 & 0 & 0 \\ 0 & 1 & 0 & 0 & 0 & 0 \\ 0 & 0 & 1 & 0 & 0 & 0 \end{vmatrix} \begin{vmatrix} x_1 \\ x_2 \\ x_3 \\ x_4 \\ x_5 \\ x_6 \end{vmatrix} + \begin{vmatrix} 0 \\ 0 \\ 0 \\ 1 \\ 0 \\ 0 \end{vmatrix} | \, u \, | \qquad (43)$$

The equation (43) represent that picking robot arm is a typical nonlinear multivariable system with multiple input (x_1, x_2, x_3)and multiple output(u_1, u_2),the system own a strong coupling between the variables and this coupling effect changes constantly with the movement of picking robot arm.

III. DYNAMICS MODELING OF PICKING ROBOT ARM SPACE

The joints are the core component of space manipulator joints and they play an important role in the mechanical arm dynamics. They can not only do plane motion but also can take complex spatial motion in the joint space. The position X of 3 - DOF picking robot arm depends on the three joint variables, and these joint variables are also called 3 d joint vector q. All of these joint vectors q constitute the joint space. Picking robot arm assignments is finished in rectangular coordinate space, namely, so we describe the joint position in the rectangular coordinate space and we call this space as picking space. Kinematics equation $X = X(q)$ is mapping form the joint space to picking space, but the kinematics inverse solution come from the mapping in joint space. In joint space and picking space, dynamics equations have different expression form, there exist the certain corresponding relationship between the representations.

(1). Dynamic joint space equations

Understanding the dynamic characteristics of the joints accurately and comprehensively is the key to correct analysis and simulation the movement characteristics of picking space, but establishing accurate dynamic model of the joints is the basis on designing, analysis and controlling picking robot arm system. Now we can write equation (28),(30), (31), (34), (35), (38), (39) as matrix form

$$\tau = D(q)\ddot{q} + H(q,\ddot{q}) + G(q) \qquad \textbf{(44)}$$

Where $\tau = \begin{bmatrix} \tau_1 \\ \tau_2 \\ \tau_3 \end{bmatrix}$; $q = \begin{bmatrix} q_1 \\ q_2 \\ q_3 \end{bmatrix}$; $\dot{q} = \begin{bmatrix} \dot{\theta}_1 \\ \dot{\theta}_2 \\ \dot{\theta}_3 \end{bmatrix}$; $\ddot{q} = \begin{bmatrix} \ddot{\theta}_1 \\ \ddot{\theta}_2 \\ \ddot{\theta}_3 \end{bmatrix}$ so

$$D(q) = \begin{bmatrix} m_1 p_1^2 + m_2 k & m_2(p_2^2 + l_1 p_2 \cos\theta_2) & m_2 p_2^2 \\ m_2(l_1 p_2 \cos\theta_2 + p_2^2) & m_3 p_3^2 + m_2 h & m_3(l_3 p_2 \cos\theta_3 + p_1^2) \\ m_3(p_1^2 + l_2 p_3 \sin\theta_3) & 2l_2 p_1 c\theta_2 + 3l_3 p_1 \cos\theta_3 & m_3 p_3^2 \end{bmatrix} \qquad \textbf{(45)}$$

Where $h = l_1^2 + l_2^2 + 2l_1 p_2 \cos\theta_3$, $k = l_1^2 + l_2^2 + 2l_1 p_2 \cos\theta_2$

$$H(q,\dot{q}) = \begin{bmatrix} -m_2 l_1 p_2 \sin\theta_2 \dot{\theta}_2 - 2m_2 l_1 p_2 s\theta_2 \dot{\theta}_1 \dot{\theta}_2 \\ m_2 l_1 p_2 \sin\theta_2 \cos\theta_3 \dot{\theta}_1^2 + \\ -m_3 l_1 p_2 \sin\theta_3 \dot{\theta}_3 - 3m_1 l_2 p_2 \cos\theta_2 \dot{\theta}_1 \dot{\theta}_3 \end{bmatrix} \qquad \textbf{(46)}$$

$$G(q)=\begin{bmatrix}(m_1p_1+m_2l_1)g\sin\theta_1+m_2p_2g\sin\theta_3\\ m_3p_1g\sin\theta_2\\ (m_2p_2+m_3l_2)g\sin\theta_2+3m_2p_2g\sin\theta_3\end{bmatrix} \qquad (47)$$

Equation (44) is the general structure form of the dynamics equation in joint space, which represents the relationship between the joint torque and joint variables, function velocity and acceleration. In view of the picking robot arm own joints form, the $D(q)$ denotes $n\times n$ positive definite symmetric matrices, it is the inertia matrix, the $H(q,\dot{q})$ denotes $n\times 1$ centrifugal force and Coriolis force vector, the $G(q)$ denotes $n\times 1$ gravity vector, it relates to the form q of picking robot arm .

(2). Dynamic equations of picking space

Corresponding to the dynamics equation in the joint space, the dynamics equation of picking robot arm in the Cartesian space can be represented by rectangular coordinate variables, namely, the dynamics equation of picking robot arm in Cartesian space can be represented by position vector X of picking grippers. To making full use of space dynamic, we can make picking gripper to the expected position, trip, or to achieve a predetermined picking action, and can also get the space predetermined trajectory. As mentioned above, the relationship between the picking force F and picking gripper acceleration $\ddot{x}$ can be represented as

$$F=M_x(q)\ddot{X}+U_x(q,\dot{q})+G_x(q) \qquad (48)$$

Where $M_x(q)\ddot{X}$ denotes the inertia matrix of picking space, $U_x(q,\dot{q})$ denotes the centrifugal force vector, $G_x(q)$ denotes the Coriolis force vector, gravity vector, F denotes the generalized picking force vector. The corresponding relationship between joint space dynamic equation and picking space dynamics equation can be solved by the relationship between the generalized picking force F and the generalized joint force τ and the relationship between the velocity and acceleration of picking space and joint space

$$\tau=J^T(q)F \qquad (49)$$

$$\begin{cases}\dot{X}=J(q)\dot{q}\\ \ddot{X}=J(q)\ddot{q}+J(q)\dot{q}\end{cases} \qquad (50)$$

IV. LQR ZONE CONTROLLER DESIGN OF PICKING ROBOT ARM

(1). Design on the picking Zone control

According to the dynamic model equation of apple picking robot arm and the above described controlling strategy, the motion control space can be broken into two corresponding secondary range, the stretching area which the main movement space including approaching the mature apple position, the picking areas which main the movement space including picking mature apple position. Because the stretching mechanism in the large range of motion in preparation for fetching mature apple alike mankind stretching process, that is to say, first driving the upper arm by the rotation shoulder, then driving the forearm by the elbow joint until picking gripper stretching to grab area. In the whole picking action, the potential energy of picking forearm and picking gripper increases gradually, when the picking gripper reach picking district, the shoulder joint and elbow joint can reach into the servo steady state. From the energy increase in stretching process and the picking robot arm control laws, the total energy in the process of movement is

$$E\left(\theta,\dot{\theta}\right)=\sum_{i=1}^{3}K_i+\sum_{i=1}^{3}P_i \qquad \textbf{(51)}$$

In order to ensure the energy increases in the whole stretching action, the following equation must be established as

$$E\left(\theta,\dot{\theta}\right)\geq 0 \qquad \textbf{(52)}$$

By the characteristics of the ant symmetric matrix,

$$E\left(\theta,\dot{\theta}\right)=\dot{\theta}\tau \qquad \textbf{(53)}$$

To meet the increasing energy inequality conditions, the control torque of stretching area is

$$\tau_i=\mathrm{sgn}\left(\dot{\theta}_i\right)N_i \qquad \textbf{(54)}$$

Where sgn( ) denotes the symbolic function, N_i denote the additional force, $N_i \geq 0$, i=2,3.

The basic idea of stretching control is that the system energy should be increased in the control process. Actually, we could design controller for the shoulder joint drives and the wrist drives to ensure the additional force decreases with the increase of energy and stretch smoothly to picking area.

b. The LQR control of picking robot arm

In order to deal with the control system simply, the system equation will be discretized. The common discretization methods including Euler method, linear differential complement, zero-valet maintain, zero pole assignment and double linear differential complement [16-18]. As a kind of multivariable, coupling nonlinear system, Euler method is suitable for the nonlinear systems with time-delay [19], so the control equation on accurate discretization is represented as

$$\begin{cases} x(k+1) = Gx(k) + Hu(k) \\ y(k) = Gx(k) \end{cases} \qquad (55)$$

Where $G = \exp(\bar{A}T)$, $H = \int_0^T \exp(\bar{A}(T-\tau))\bar{B}dt$, T denotes the sampling period of discretization, k=0,1,2,….,n. The Linear Quadratic Regulator called LQR controller should judge whether if the system is controlled firstly. Generally, we judge the controllability using the system controllability matrix M_c= ［$H\ \ GH\ \ G^5H$］ is full rank or not. If the controllability matrix is a full rank, the system can be controlled, otherwise the system can be not controlled. By calculating we know that Mc rank is 6, means the full rank matrix, it represents that the picking robot arm system is controllable. In this system, we can achieve stability using configuring system poles through state feedback variables（$\theta_1, \theta_2, \theta_3, \dot{\theta}_1, \dot{\theta}_2, \dot{\theta}_3$）and gain the control strategy of linear feedback controller shown as Figure 2.

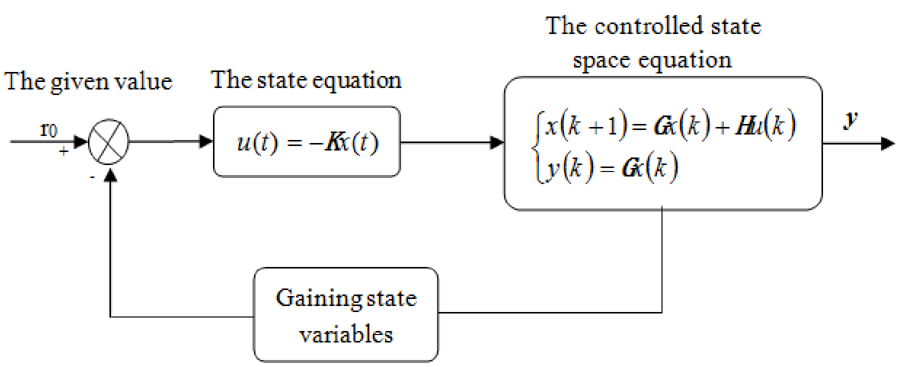

Figure. 2 Linearity feedback controller strategy of the picking system

We can obtain the state feedback variables by the servo motor encoder, the encoder used for measuring the angle and its own difference. According to the literature experience [19-20], we can apply the classical effective control strategy directly the quadratic optimal control strategy based on the linear model. So the state space model is applied to design the LQR controller in the picking area. By the conclusion [21], we can gain the linear quadratic optimal control law, the controller state equation is

$$u(t) = -Kx(t) \qquad (56)$$

According to the simplified system state equation $\dot{x} = Ax + Bu$ from the equation (43), we can obtain the value of k in the optimal control vector matrix $u(t) = -Kx(t)$ which makes the performance index J is minimal.

$$J = \int_0^\infty (x'Qx + u'Ru)\mathrm{d}t \qquad (57)$$

Where Q denotes positive definite or positive semi-definite Hermitical and real symmetric matrix, R denotes positive definite Hermitical or real symmetric matrix. Matrix Q and R determine the relative weighting factor of the error and the energy loss, we can solve the best stability control problem of picking robot arm by substituting the equation (56) into the simplified equation of state

$$\dot{x} = Ax + BKx = (A - BK)x \qquad (58)$$

In the derivation equation, it is assumed that $A - BK$ matrix is stable, that is to say, all the characteristic roots of $A - BK$ have negative real part or on the left half complex plane, substitute equation (56) into the equation (57)

$$J = \int_0^\infty (x'Qx + x'K'RKx)\mathrm{d}t = \int_0^\infty x'(Q+K'RK)x\mathrm{d}t \qquad (59)$$

According to the parameter optimal problem [20-21]

$$x'(Q+K'RK)x = -\frac{d}{dt}(x'Px) \qquad (60)$$

The P in the equation (60) is the Hermitical positive definite and symmetric matrix. So

$$x'(Q+K'RK)x = -\dot{x}'Px - x'P\dot{x} = -x'[(A-BK)'P + P(A-BK)]x \qquad (61)$$

Comparing on both side of equation (61) and known that equation is established for any x, so

$$(A-BK)'P + P(A-BK) = -(Q + K'RK) \qquad (62)$$

According to the Lyapunov second order method [22],if $A - BK$ is a stable matrix, there must exist a positive definite matrix satisfying the equation (62). Determining the element of P and testing whether the positive definite by this method, if the picking robot arm system is stable, we can always seek a positive definite matrix P satisfy the equation and solve the equation. the performance index of equation (59) can be calculated as

$$J = \int_0^\infty (x'Qx + x'K'RKx)\mathrm{d}t = -x'Px\Big|_0^\infty = -x'(\infty)Px + x'(0)Px(0) \qquad (63)$$

Because of all the characteristic roots of $A - BK$ own negative real part, so $x(\infty) \to 0$

$$J = x'(0)Px(0) \qquad (64)$$

So the performance indicators can be obtained according to the initial conditions $x(0)$ and the matrix *P*.

We can solve the solution of quadratic optimal control problem by certain steps. Because the matrix *A* is a positive definite Hermitical or symmetric matrix, it can be represented n as $R = T'T$, the matrix *T* is not a singular matrix. The equation (62) can be represented as

$$(A' - B'K')P + P(A - BK) + (Q + K'T'TK) = 0 \qquad (65)$$

We need to calculate the minimum of *J* to *K*, namely the minimum of $x'[TK - (T')^{-1}B'P]'$ $[TK - (T')^{-1}B'P]x$ to *K*, for the result of this equation is not negative, it can search the minimum when it is zero, namely, it can gain the minimum when the equation $TK = (T')^{-1}B'P$ is found. so

$$K = T^{-1}(T')^{-1}B'P = R^{-1}B'P \qquad (66)$$

equation (66) give the best matrix *K*, so when the performance of the quadratic optimal control problem is defined by equation (57), the optimal control law is linear and we can obtain it from $u(t) = -Kx(t) = -R^{-1}B'Px(t)$. The equation (66) must satisfy the following degradation equation

$$A'P + PA - PBR^{-1}B'P + Q = 0 \qquad (67)$$

The equation (67) is called the degenerate matrix rickety equation, its design steps is included that first solving the degradation of rickety equation to obtain the matrix is *P*, if there is the positive definite matrix *P*, the system is stable, namely, the matrix $A - BK$ is stable, then we can obtain the best matrix *K* by generating the matrix into the equation (66).

V. THE SIMULATION EXPRIMENTS AND ANALYSIS

(1). Experimental methods and steps

a. Establish relation curve s of kinematics mathematic model

Firstly, with the aid of the necessary translational and rotational movement, we can make the base coordinate system superposes with the fixed coordinate system and establish the correspondence relationship between the measurement data and motion equations, Then gain the picking space coordinates of picking grippers such as A_8 (-900,492,-871) shown as table 2 and substitute the coordinate values into the equation (49) and (50),we can obtain the positions of picking robot arm joints, then set the displacement drive of joint using a STEUP function and set 5s simulation time and 50 simulation steps and writing Matlab program to observe the movement simulation for picking robot arm ,we can gain the relation curves of kinematics mathematical model shown in figure 3, figure 4, figure 5 to the simulation.

(2) Establish unit step response curve in picking area

We can solve continuous time of linear quadratic controlling problem make use of the Matlab command [K，P，E]=LQR(A，B，Q，R), and can also solve the related rickety equation, This command is applicable to calculate the optimal feedback gain matrix *K*, and produce performance metrics and make it to tiny feedback control law on the condition of constraint equation $\dot{x} = Ax + Bu$. In order to meet the requirements of stability control，the corresponding weight coefficient of the controlled variables and the weight values matrix is generally larger, and only when the weight values matrix is generally larger, the system can quickly achieve a stable state to suppress the fluttering. The value of the matrix *Q* in a certain range is larger, the time to regulate the system is shorter, but it is not too large, while enlarge to a certain extent it can lead to larger fluttering and be not conducive to stable. Because the angular velocity of joint has bigger influence on the control system, the value of the matrix *Q* and *R* is the following

$$\boldsymbol{Q} = \begin{vmatrix} 100 & 0 & 0 & 0 & 0 & 0 \\ 0 & 100 & 0 & 0 & 0 & 0 \\ 0 & 0 & 110 & 0 & 0 & 0 \\ 0 & 0 & 0 & 100 & 0 & 0 \\ 0 & 0 & 0 & 0 & 100 & 0 \\ 0 & 0 & 0 & 0 & 0 & 100 \end{vmatrix} \qquad R = \begin{vmatrix} 20 & 0 \\ 0 & 20 \end{vmatrix}$$

Make use of the value of the matrix *Q* and *R*, we can solve the optimal state feedback matrix, then we can solve the optimal state feedback gain matrix K_{LQR}=[31.1208 -18.171 3.2670 4.2683 -2.6939 -7.0642] according to the *A* and *B* in the equation (43) and the known testing parameter data after we choose the weight matrix. Then we can validate the unit step response of the designed LQR controller using the Matlab program shown as Figure 4.

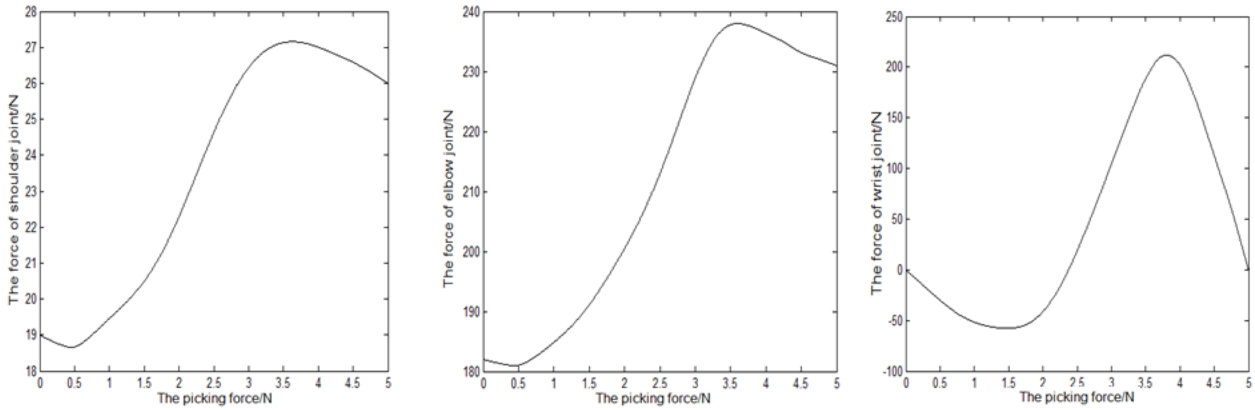

Figure.3 The relationship between picking force and joints force

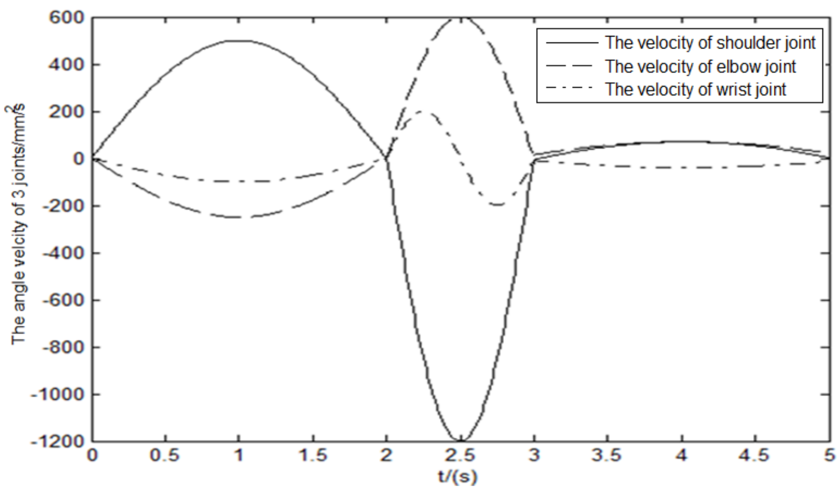

Figure. 4 The curve of joint velocity between picking space and joint space

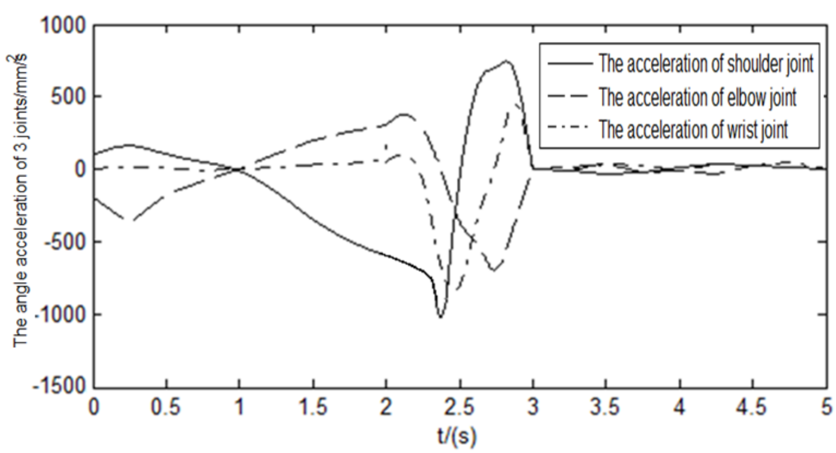

Figure.5The curve of joint acceleration between picking space and joint space

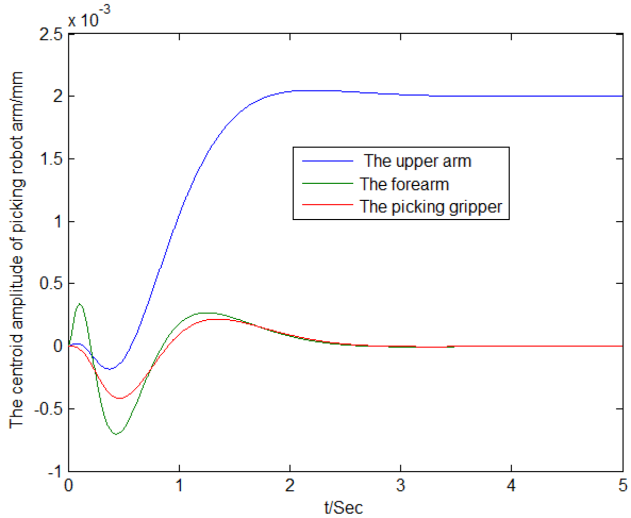

Figure.6 Unit step response curve of picking space of picking-arm

(3). Experimental results and analysis

The picking application is based on a simple pick operation using the setup described in Figure 6. This is a simplification of a real environment to show the profits of the LQR zone control architecture. As can be seen in Figure 6, there are 3 joint positions err to pick the apple: 2mm, 0.3mm, 0.15mm. It is possible to pick more than one apple in the scene. However, to simplify the movement, the system has been validated with only one apple. Each movement position is marked. The picking movements consist of changing the position of the object picked on the scene to another position. The picking robot arm starts in 0 °. Three different joints velocities are designed (Figure. 4). Regarding the picking movement, the average uncertainty is in both cases around 15% or so. This means that the error decreases from the one obtained in the picking training. These success rates are similar or greater to the ones obtained in with a shared control of a mobile crane, however, in the future, this uncertainty should be reduced by improving the picking performance. Picking movement will be used to improve the control of the robot arm in grasping tasks where daily objects with different heights are used. The use of three arms joints can be implemented to obtain a larger range of daily objects that can be picked. Also, the use of visual picking strategies could assist the recognition of the different apples. In this sense, it is planned to perform picking operation in order to create more useful applications for them and obtaining a real feedback of their special needs. Figure 4 and Figure 5 represents that the joint velocity and acceleration are driven by disturbances from step function, this picking action can change relatively smooth in the process of picking robot arm movement, but the joint velocity and acceleration appear to sudden change nearby the 2s and 3s. In order to reduce the instability in the process of the picking robot arm movement, we should correct the centrifugal force, the Coriolis force vector and gravity vector to reduce driving joints in turn and to enhance the overall operation stability. Figure 3 represents that joint force and picking force curve can change without mutation in the case of external environment. It also represents that picking robot arm can move smoothly and have no vibration in the process of picking movement. By comparing picking robot arm joint force curve, we can gain the shoulder joint torque is the largest, so on the beginning of picking robot arm , the longest shoulder joint is, the biggest force providing. Elbow and wrist joints are the second. Simulation results represent the correctness to the kinematics equation in picking space. After correcting the centrifugal force, Coriolis force vector and gravity vector, we can gain the result from the unit step response curve of the picking area shown as Figure 6, the most vibration quantity of upper arm is about 4.6 mm, the fitting time for forearm is less than 2s, As for the end actuator picking grippers, the vibration quantity is the minimum through the same direction vibration as the forearm approximately, it can tend to be stable in about 1.5s, Three joints eliminated vibration in the picking space and reached the basic stability state in 2s or so with the smaller vibration quantity less than 4.6 mm.

VI. CONCLUSIONS

This paper is dedicated to solve the poor stability of picking robot arm in picking apples and reduce the fluttering problems. A novel robust LQR zone control algorithm featuring finite-time parameter estimation for humanoid robot arm is presented. The picking feature introduced both in the picking and estimation scheme provides two-fold benefits. One is to provide significant levels of robustness against bounded disturbance both within the picking error and estimation error. The second benefit is that finite-time convergence in the parameter estimation error can be guaranteed given sufficient instability condition in the picking movement. According to the design of energy zone controller based on LQR and the simulation, the upper arm, forearm and picking grippers can reach the stability state in the interval of 2s or so, when there exit input disturbance. The overshoot amount is the relatively small and the system has the strong robust stability and level off quickly. Moreover, we establish the analysis and research on the robust performance by the LQR algorithm energy zone strategy to ensure the reliability of the control strategy.

Acknowledgements

This work is funded by Technology Innovation Foundation of Northwest A&F University (No.QN 2013051 and No.2014Yb068) and Doctor Scientific Research Startup Project (No.2013BSJJ106).

REFERENCES

[1] I. Payo, V. Feliu, O.D. Cortazar, “Force control of a very lightweight single-link flexible arm based on coupling torque feedback”, Mechatronics Vol.19 ,2009,pp.334–347.

[2] M. Madani, M. Madani, M. Moallem, “Hybrid position/force control of a flexible parallel manipulator”, Vol.348, 2011, pp.999–1012.

[3] Chen C., Ong S., Nee A., Zhou Y, “Haptic-based interactive path planning for a virtual robot arm”, International Journal on Interactive Design and Manufacturing,Vol.4,no.2, 2010,pp. 113-123

[4] Alessandro Shimabukuro,“No deal in space: A bargaining model analysis of U.S. resistance to space arms control”, Space Policy,Vol.30,2014, pp.13-22

[5] Damianou C, Ioannides K, Milonas N, “Positioning device for MRI-guided high intensity focused ultrasound system”, International Journal of Computer Assisted Radiology and Surgery, Vol.2,no.6, 2008,pp. 335-344

[6] Decker M D R, Dreier T, Fischer M, Gutmann M, Ott I, Spiecker G D, “Service robotics: do you know your new companion? Framing an interdisciplinary technology assessment”, Poiesis & Praxis: International Journal of Technology Assessment and Ethics of Science. Vol.8,no.1, 2011,pp. 25-44

[7] Efe M, “ADALINE based robust control in robotics: a Riemann-Liouville fractional differ integration based learning scheme”, Soft Computing - A Fusion of Foundations, Methodologies and Applications. Vol.13,no.1, 2009,pp. 23-32

[8] M.N. Mahyuddin, S.G. Khan, G. Herrmann,“A novel robust adaptive control algorithm with finite-time online parameter estimation of a humanoid robot arm”, Robotics and Autonomous Systems,Vol.62 ,2014,pp.294–305

[9] Feng J., Gao F., Zhao X., Yue Y., Liu R,“ A new macro-micro dual drive parallel robot for chromosome dissection”, Journal of mechanical science and technology, Vol.26,no.1, 2012,pp. 187-194

[10]Fujioka K., Geis P., Saito M., Matsuoka H., “Visualization of yeast single-cells on fabric surface with a fluorescent glucose and their isolation for culture, Journal of industrial microbiology \& biotechnology”, Vol.34,no.10, 2007,pp. 685-688

[11] Hagras H, Colley Mn, Callaghan V, Carr-West M, “Online Learning and Adaptation of Autonomous Mobile Robots for Sustainable Agriculture, Autonomous Robots”, Vol.13,no.1, 2002,pp. 37-52

[12] Takahiro Endo, Haruhisa Kawasaki,“Bending moment-based force control offlexible arm under gravity”, Mechanism and Machine Theory,Vol.79,2014,pp.217–229

[13] Harper C., Virk G, “ Towards the Development of International Safety Standards for Human Robot Interaction, International Journal of Social Robotics, Vol.2,no.3, 2010,pp. 229-234

[14] He B, Liu G, Ji Y, Si Y S, Gao R,“Auto Recognition of Navigation Path for Harvest Robot Based on Machine Vision”, Springer Boston, 2011,pp.138-147

[15] Katharina Beier*,Detlef Ehlert,“Methods for evaluation of picking performance of chamomile (Matricaria recutita L.) harvesters. Part I:Comparison of established methods” Journal of Applied Research on Medicinal and Aromatic Plants,Vol.1,2014,pp.e1–e7

[16] Lee S Lee Y, Park B, Lee S, Han C, “ MFR (Multipurpose Field Robot) for installing construction materials, Autonomous Robots”, Vol.22,no.3, 2007,pp. 265-275

[17] Lee T, Hudson S, Chang J Y, “Auto-detection micro-controller-based autonomous band wrapping system for targeted pest control”, Microsystem Technologies, Vol.16,no.1, 2010,pp. 227-238.

[18] G. Sen Gupta and S.C. Mukhopadhyay, “A Triangular Targetting Algorithm (TTA) for Motion Control of Wheeled Mobile Robots”, Proceedings of the International Conference on Emerging Mechanical Technology – Macro to Nano (EMTM2N 20007), February 16-18, 2007 at Pilani, India, pp. 204-209.

[19] Monta M., Kondo N. and Ting K.C,“ End-Effectors for Tomato Harvesting Robot, Artificial Intelligence Review”, Vol.12,no.1, 1998,pp.11-25.

[20] S.C.Mukhopadhyay and G. Sen Gupta, “Sensors and Robotic Environment for Care of the Elderly”, Proceedings of IEEE International Workshop on Robotic and Sensors Environments, Ottawa, Canada, 12-13, 2007, pp. 68-73.

[21] Naveen K, Jin-Hwan B, Vikas Pand J C,“Tracking control of redundant robot manipulators using RBF neural network and an adaptive bound on disturbances, International Journal of Precision Engineering and Manufacturing”, Vol.13,no.8, 2012,pp.1377-1386.

[22] G. Sen Gupta, S.C.Mukhopadhyay and J. R. French, Wireless Communications and Control Module of a Web-Enabled Robot for Distributed Sensing Applications, Proceedings of IEEE International Instrumentation and Measurement Technology Conference, Victoria, Canada, May 12-15, 2008, pp. 393-398.

[23] Andrés Úbeda, Eduardo Iáñez∗, José M. Azorín,“Shared control architecture based on RFID to control a robot arm using a spontaneous brain–machine interface”, Robotics and Autonomous Systems, Vol.61,2013,pp.768–774.

[24] František Kumhála,Miroslav Kavka, Václav Prošek,“Capacitive throughput unit applied to stationary hop picking machine”, Computers and Electronics in Agriculture,Vol.95,2013,pp.92–97.

[25] G. Sen Gupta, S.C. Mukhopadhyay, S. Demidenko and C.H. Messom, “Master-slave Control of a Teleoperated Anthropomorphic Robotic Arm with Gripping Force Sensing”, IEEE Transactions on Instrumentation and Measurement, Vol. 55, No. 6, pp. 2136-2145, December 2006.

[26] McCarthy C. L, Hancock N. H and Raine S. R, “Applied machine vision of plants: a review with implications for field deployment in automated farming operations”, Intelligent Service Robotics, Vol.3,no.4, 2010,pp. 209-217